

Temperature Control of Electric Furnace Using Adaptive Lag Compensator Based on Improved Gorilla Troops Optimization: Towards Energy Efficiency

Mohamed Roshdy, Tarek Hassan Mohamed, Asmaa Fawzy

Electrical Engineering Department, Faculty of Energy Engineering, Aswan University, Aswan 81528, Egypt

Abstract: A lot of study has been done in recent years to increase the energy efficiency of engineering systems. It is essential to create effective temperature control systems since electric furnaces (EF) account for a significant portion of energy usage. The majority of established techniques need accurate system parameter knowledge/sufficient data. Nevertheless, in the case of dynamic parameter variation, these methods might not operate as well. In many industrial applications, controlling the temperature of EFs is regarded as one of the key problems. In this paper, an EF temperature system with an adaptive lag compensator is proposed. Application of artificial gorilla troops optimization (GTO) supported by the balloon effect (BE) (GTO+BE) identifier estimates the integral coefficient of the adaptive lag compensator for temperature control purposes. Due to the low efficiency of the objective functions employed in ordinary optimization, the BE identifier is used to raise the optimization technique's objective function's efficiency and the controller's ability to handle system problems, both of which rise as a result. The issue of parameter fluctuations and step disruption is intractable for conventional controls like PID controllers. The proposed technique adaptive lag compensator based on GTO+BE is compared with the modified flower pollination algorithm (MFPA)-based PIDA, and MFPA-based PID controllers. From the results, the proposed adaptive lag compensator with GTO+BE gives the best dynamic performance of an EF temperature system with the minimum overshoot, rise time, and settling time.

Keywords: Adaptive lag compensator; balloon effect; electric furnace; gorilla troops optimization (GTO); modified flower pollination algorithm (MFPA); temperature control.

List of abbreviations

HFs: heating furnaces	MLP: multi-layer perceptron
PID: proportional-integral-derivative	GWO: grey wolf optimization
ZN: Ziegler-Nicholes	WOA: whale optimization algorithm
CC: Cohen-Coons	SCA: sine cosine algorithm
SMCs: sliding mode controllers	PSS: power system stabilizer
RCC: A robust composite control	ITSE: integral time square error
PIDA: PID accelerated	TID: tilt-integral-derivative
EFT: electrical tube furnace	BE: balloon effect
MFPA: modified flower pollination algorithm	GTO: gorilla troops optimization
FOMPC: fractional order model predictive control	TL: Tyreus Luyben's
MRFO: Manta ray foraging optimizer	TC: temperature control
ENMSS: extended non-minimal state space	EF: electric furnace

1. Introduction

Industrial goods, such as those involving metal melting, polymerization, drying, and other physical-chemical processes, commonly employ industrial heating furnaces (HFs) [1], [2]. Electric HF temperature processes are characterized by great inertia, time delay, and unpredictability, which makes

it difficult for conventional control techniques to fulfill the growing expectations for control performance improvement that directly impact product quality [3], [4]. Traditional control, such as proportional-integral-derivative (PID), is widely used because of its ease of use and simplicity [5], [6]. One of the well-known, efficient techniques is the PID controller, which continues to be a common research topic and application in industrial process control. However, the PID controller may take a long time to reach a steady state for processes with high inertia and time delays, and it cannot adequately meet the growing demands for control performance. Ziegler-Nicholes (ZN) and Cohen-Coons (CC) techniques are considered to be the most preferred for tweaking the standard PID approach [7].

A tempered glass furnace system was designed using two sliding mode controllers (SMCs) to manage the temperature of the glass plate, the upper and lower walls, and the furnace to a common desired temperature [8]. For the electrical tube furnace (ETF), a robust composite control (RCC) approach offered accurate and reliable temperature tracking performance [9]. On the electric furnace (EF) temperature control (TC) system, the PID accelerated (PIDA) controller design based on the modified flower pollination algorithm (MFPA) [10], an improved approach of extended non-minimal state space (ENMSS) fractional order model predictive control (FOMPC) [11], is tested.

The ZN and TL (Tyreus Luyben) tuning techniques are applied to obtain the three PID parameters. For the given system, LQR and PID (using ZN and TL) control techniques provide better performance [12]. For the EF, a fuzzy PID controller is created [13], [14]. For the electrical heater furnace problem, the PID decoupling control approach based on the DRNN neural network setting was proposed under Jacobian information identification of the DRNN neural network [15]. The PID controller parameters were adjusted by the Nelder Mead optimization process to function in an EF-TC system [16]. To address the low precision, long rise time, and settling time of the controller, a PID controller based on genetic algorithms was introduced for regulating the EF's temperature [17]. For an electrical heating furnace system, a predictive fuzzy-PID controller reduced overshoot, minimized stability time, and increased control precision [3]. An algorithm for fuzzy control has two stages. The control variable is selected by the first-stage controller using the deviation data of the controlled variable. The second-stage controller is responsible for changing the control variable, which comes from the first-stage controller, by adding new process parameters. Next, the control algorithm is highly robust, accurate, and so on [18], [19]. Insufficient temperature control in an EF leads to increased power losses. As a result, consistent temperature control is considered a method to lower the EF's overall energy consumption.

In many industrial applications, gains of conventional controllers have been adaptively tuned using optimization approaches like the artificial gorilla troops optimization (GTO) [20]. The optimum gains of the cascaded PI-FOPID controller are fine-tuned using GTO to improve the frequency response of a hybrid microgrid system [21], [22]. Moreover, GTO trains a multi-layer perceptron (MLP) and its result is compared with grey wolf optimization (GWO), the whale optimization algorithm (WOA), and the sine cosine algorithm (SCA) [23],[24][25]. The complicated nonlinear variables of current voltage and power voltage make it challenging to extract the characteristics of solar photovoltaic generating systems. To extract parameters from various PV models, a new implementation of the GTO method was developed [26]. To control energy consumption in DC-AC hybrid distribution networks, GTO was presented. It was suggested to put in place an energy management system that accounts for load demand, distributed generation, and battery charge status [27], [28]. The GTO algorithm determines the best tuning parameters for a power system stabilizer (PSS) unit. The integral time square error (ITSE) is used as a fitness function, which should ideally be reduced. The investigation of a single-machine

approach as a model for the infinite bus uses four different controllers tilt-integral-derivative (TID), PID, lead-lag, and FOPID. The TID exhibits a greater performance response [29], [30].

On the other hand, utilizing nominal parameters when building the objective function while considering the zero-load disturbance is one of the drawbacks of using classical techniques in the adaptive control approach. As a result, when disturbances and parameter changes occur, the performance will be weak. To address this problem and increase the optimization algorithm's sensitivity to both disturbances and parameter changes, this paper suggested adding a balloon effect (BE) modification [31], [32].

This paper proposes an EF temperature system for TC with an adaptive lag compensator based on GTO+BE. GTO+BE is used to estimate the adaptive lag compensator's integral coefficient. To determine the impact of the suggested method on the system under investigation, the suggested control technique is compared with MFPA-based PIDA and MFPA-based PID controllers. It is anticipated that the dynamic performance of an EF temperature system will be enhanced in terms of minimum overshoot, rise time, and settling time as a result of the superiority and accuracy of GTO+BE.

The rest of this paper is structured as follows: There is an EF temperature system in Section 2. Section 3 discusses the GTO. In Section 4, the BE is showcased. In Section 5, the suggested control system is described. Section 6 examines the simulation results. Section 7 presents the conclusions.

2. Electric Furnace Temperature System

Figure 1 depicts the schematic diagram of the EF temperature system, which includes an EF, a controller, a thermocouple, and a heater to regulate the furnace's temperature [10]. In this figure, r , U , y , and R represent the input voltage, the controller's output voltage, the thermocouple's output voltage, and the armature resistance, respectively. The second-order transfer function plus time delay describes the EF temperature system as follows:

$$G(s) = \frac{b_0}{a_2 s^2 + a_1 s + a_0} e^{-Ds} \quad (1)$$

$$G(s) = \frac{0.15}{s^2 + 1.1s + 0.2} e^{-1.5s} \quad (2)$$

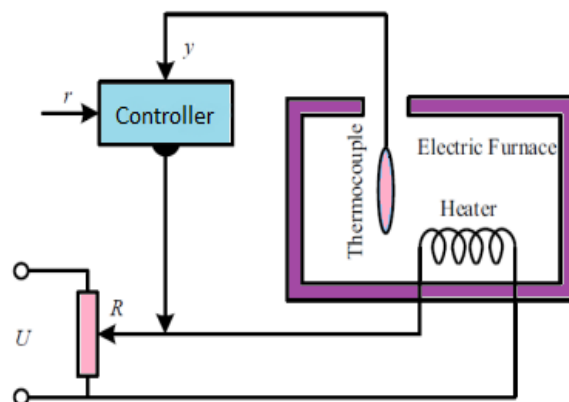


Figure 1. EF temperature system [10].

The first-order Pade approximation estimates the time delay as shown in Equation (3).

$$e^{-1.5s} = \frac{1 - 0.75s}{1 + 0.75s} \quad (3)$$

Then, the transfer function of the EF temperature system will be:

$$G(s) = \frac{-0.1125s + 0.15}{0.75s^3 + 1.82s^2 + 1.25s + 0.2} \quad (4)$$

This plant model $G(s)$ is used in the control loop in Figure 2. The transfer function of the PIDA controller is [33]:

$$G_{PIDA}(s) = k_p + \frac{k_i}{s} + \frac{k_d s}{s+d} + \frac{k_a s^2}{(s+d)(s+e)} \quad (5)$$

where K_p , K_i , K_d , and K_a stand for proportional, integral, derivative, and accelerated gains, respectively. The poles of the PIDA controller (d , e) can be neglected, when $0 \ll d, e$. The PIDA transfer function can be rewritten as:

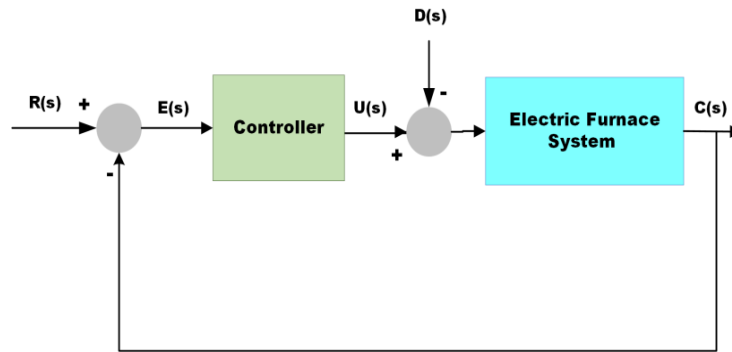


Figure 2. Closed loop electric furnace temperature control system [10].

$$G_{PIDA}(s) = k_p + \frac{k_i}{s} + k_d s + k_a s^2 \quad (6)$$

The MoFPA is utilized to design the optimal PIDA controller of the EF temperature control system [10].

$$G_{PIDA}(s) = 3.98 + \frac{0.66}{s} + 4.99s + 0.99s^2 \quad (7)$$

The block diagram in Figure 3 demonstrates the MFPA-based PIDA controller design optimization structure for the EF-TC system.

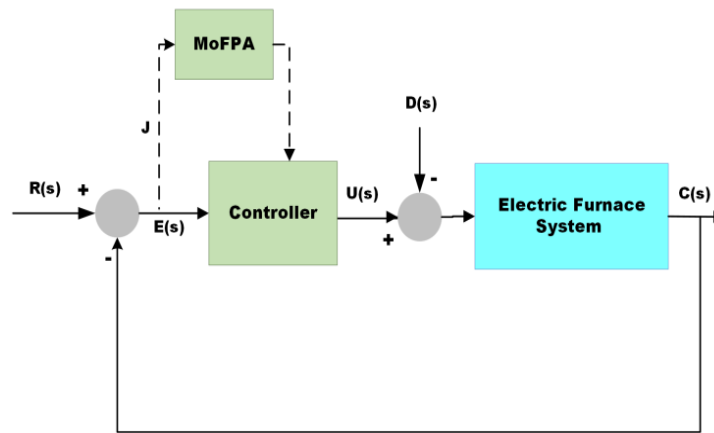


Figure 3. Block diagram of MoFPA-based PIDA controller design optimization structure [10].

3. Artificial Gorilla Troops Optimization (GTO)

It is a new metaheuristic algorithm that was motivated by the social behaviors of gorillas. The GTO method contains two phases of exploration and exploitation based on five distinct operators [27]. The exploration phase has three different operators:

- Departure for an unknown location boosts GTO exploration;
- A gorilla reaching out to others enhances the balance between exploration and exploitation;
- Departure for a known location improves the study of different optimization spaces.

The exploitation phase has two operators to improve the search performance:

- Adhere to the silverback;
- The struggle for adult females.

Figure 4 shows the flowchart of GTO that simplifies the principles of searching for a solution. Three types of solutions in the optimization space of GTO are a representation of the social life of gorillas in nature that contain the gorillas' position vector X , position vectors of the gorilla candidate GX generated in each phase improve the current solution, and the silverback yields the best solution every iteration. The number of search agents suggests only one silverback in the entire population. Gorillas tend to have a communal life. Therefore, they search for food together executing the decisions of a silverback leader. The population's worst solution is a representation of the weakest member of the gorilla group in a formulation phase, so the gorillas move near the best solution (silverback) far from the worst solution. This improves all of the gorillas' positions. The GTO method employs a number of the below-described mechanisms for optimization activities.

3.1. Exploration Phase

All gorillas are considered candidate solutions in the GTO algorithm, and the silverback gorilla is the best candidate solution at each iteration of the optimization process. In the exploration phase, three various methods have been utilized: migration to an unknown position, migration towards a known position, and migration to other gorillas. Each of these three methods is chosen based on a general process.

Equation 8 shows the three methods. $GX(t+1)$ stands for the gorilla candidate position vector in $t+1$ iteration. $X(t)$ stands for the current vector of the gorilla position. Moreover, r_1 , r_2 , r_3 , and $rand$ represent

random values from 0 to 1. The mechanism of migration to an unknown position was chosen using a parameter p that has a range of 0–1 before the optimization operation. When $\text{rand} < p$, the mechanism of migration to an unknown position is chosen. However, if $\text{rand} \geq 0.5$, the mechanism of movement towards other gorillas is chosen. However, the mechanism of migration to a known position is chosen when $\text{rand} < 0.5$. The GTO algorithm benefits greatly from each of the techniques. The first mechanism enables the algorithm to effectively monitor the entire challenge space, the second mechanism enhances the GTO's performance during exploration, and the third mechanism supports the GTO's ability to flee from local optimal regions. The upper and lower bounds of the variables are UB and LB, respectively. X_r and GX_r are two of the gorillas in the group that were randomly chosen from the entire population. The positions updated in each phase are included in one of the vectors of gorilla candidate positions that were randomly chosen.

$$GX(t+1) = \begin{cases} (UB - LB) \times r_1 + LB, \\ (r_2 - C) \times X_r(t) + L \times H, \\ X(i) - L \times (L \times (X(t) - GX_r(t)) + r_3 \times (X(t) - GX_r(t))), \end{cases} \quad (8)$$

$$C = F \times \left(1 - \frac{It}{\text{MaxIt}}\right), \quad (9)$$

$$F = \cos(2 \times r_4) + 1, \quad (10)$$

$$L = C \times l \quad (11)$$

$$H = Z \times X(t), \quad (12)$$

$$Z = [-C, C] \quad (13)$$

It represents the current value of iterations, and MaxIt represents the overall number of optimization iterations used. \cos denotes the cosine function, while r_4 represents random values updated every iteration varying from 0 to 1. L simulates the silverback leadership, which l indicates a random value in the range of -1 and 1. The position of search agent vectors changes during the exploration phase, as shown in Figure 5. A group formation operation is carried out after the termination of the exploration phase. The cost of each GX solution is determined after the exploration phase, and if the cost is $GX(t) < X(t)$, the $GX(t)$ solution is utilized in place of the $X(t)$ solution. As a result, the best solution produced during this stage is sometimes referred to as a silverback.

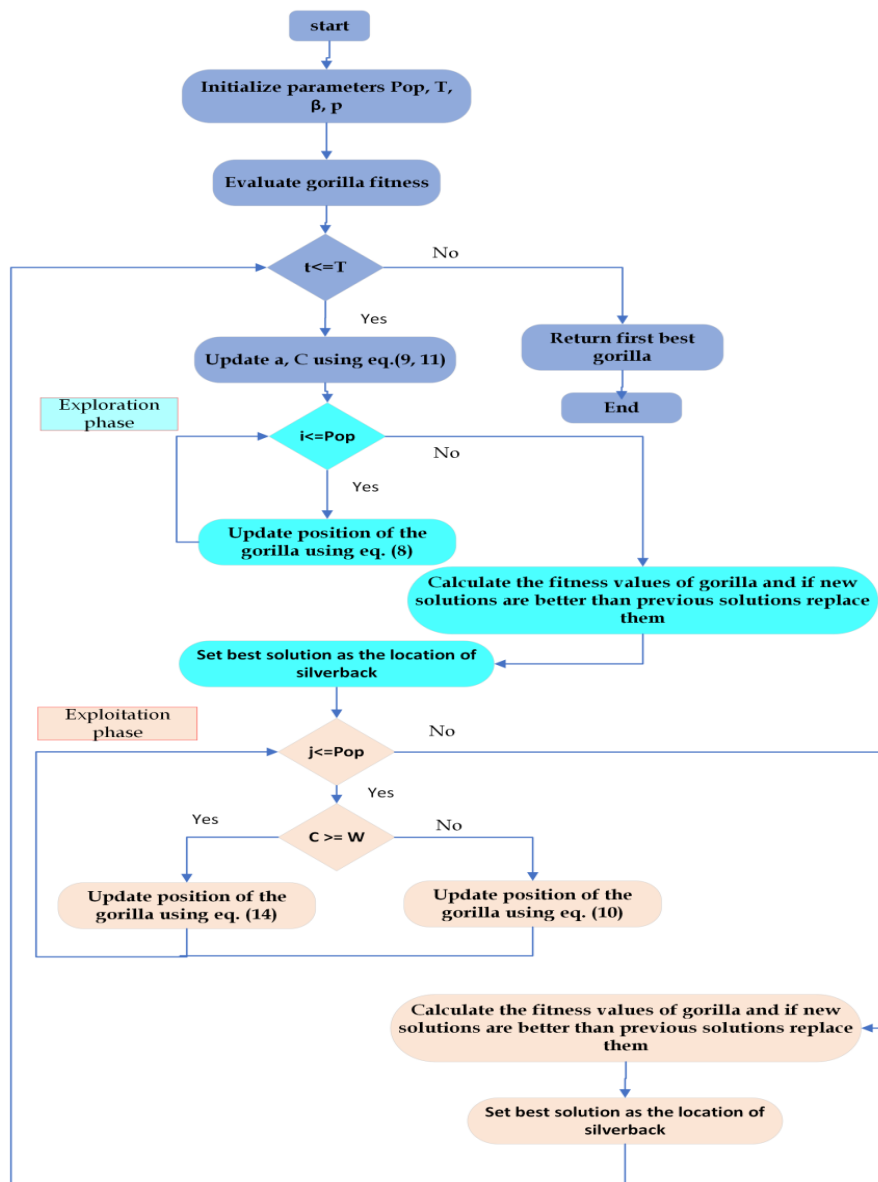


Figure 4. GTO flowchart [27].

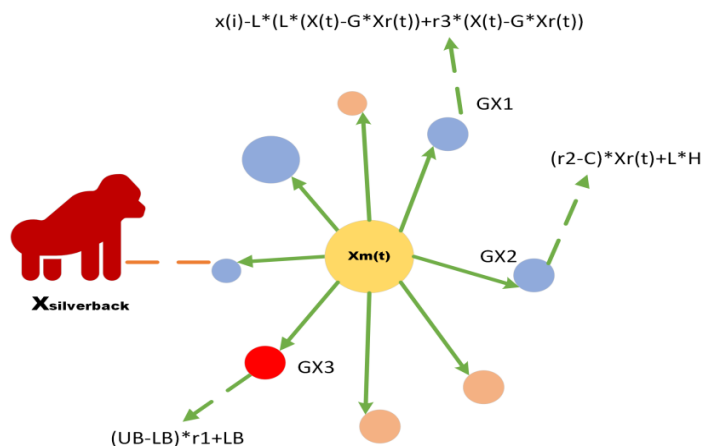


Figure 5. An illustration of overall vectors in an exploration phase [27].

3.2. Exploitation Phase

Two behaviors, competing for adult females and following the silverback, are used in this phase. The C value in Equation 9 selects between two behaviors. If $C \geq W$, the silverback mechanism is chosen; however, if $C < W$, the competition for adult females is chosen. W is a parameter that must be specified before the optimization process.

3.2.1. Follow The Silverback

Male gorillas comply with all instructions from Silverback to travel to various locations in search of food supplies. Additionally, each group member might have an impact on how the group moves. This behavior is simulated using Equation 14. This process is also demonstrated in Figure 6.

$$GX(t + 1) = L \times M \times (X(T) - X_{silverback}) + X(t), \tag{14}$$

$$M = \left(\left| \frac{1}{N} \sum_{i=1}^N GX_i(t) \right|^g \right)^{\frac{1}{g}} \tag{15}$$

$$g = 2^L \tag{16}$$

The gorilla position vector is $X(t)$, and $X_{silverback}$ denotes the silverback gorilla position vector (best solution). Moreover, $GXi(t)$ denotes the vector position of each candidate gorilla in iteration t. N stands for the total number of gorillas.

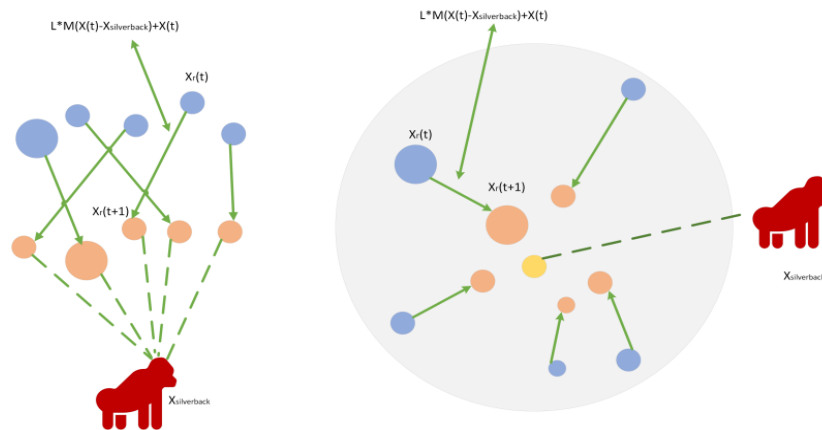


Figure 6. An example of overall vectors follows the silverback in 2D and 3D space [27].

3.2.2. Competition For Adult Females

When young gorillas reach puberty, they compete violently with other male gorillas from their group for the choice of adult females. These conflicts, which involve group members, sometimes linger for days. This behavior is simulated using Equation 17.

$$GX(i) = X_{silverback} - (X_{silverback} \times Q - X(t) \times Q) \times A \tag{17}$$

$$Q = 2 \times r_5 - 1, \tag{18}$$

$$A = \beta \times E, \tag{19}$$

$$E = \begin{cases} N_1, & rand \geq 0.5 \\ N_2, & rand < 0.5 \end{cases} \tag{20}$$

r_5 represents random values ranging from 0 to 1. The coefficient vector A determines the degree of violence in conflicts. Before the optimization operation, the parameter β must have a value. E is used to simulate the effect of violence on the dimensions of solutions. The dimensions of the problem and the value of E will be identical to random values in the normal distribution if $rand \geq 0.5$, but if $rand < 0.5$, E will be equal to a random value in the normal distribution. $rand$ represents a random number between 0 and 1. How the solutions alter is shown in Figure 7.

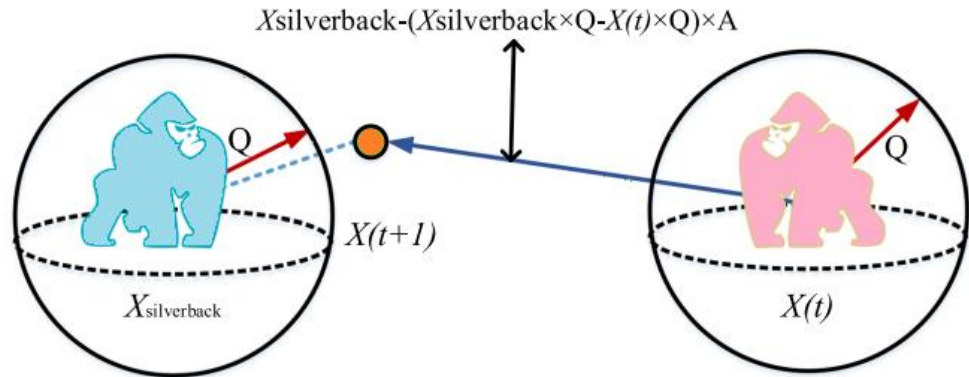


Figure 7. Example of overall vectors in the competition for adult females [27].

The best solution found across the overall population is viewed as a silverback. A group formation operation is carried out at the end of the exploitation phase, during which the costs of all GX solutions are estimated. If the costs of GX (t) and X (t) are equal, the GX(t) solution is used as the X(t) solution.

4. Balloon Effect Identifier

The expression “balloon effect” simulates how air affects balloon size. The impact of system challenges like disturbances and parameter uncertainty on $G_i(s)$ is comparable to the impact of the balloon effect. So, the balloon effect (BE) acts as an online identifier for the electric furnace temperature system. The BE identifier will affect online the objective function of the optimization strategy at any iteration as shown in Figure 8. Therefore, this technique enhances the algorithm process [31], [32].

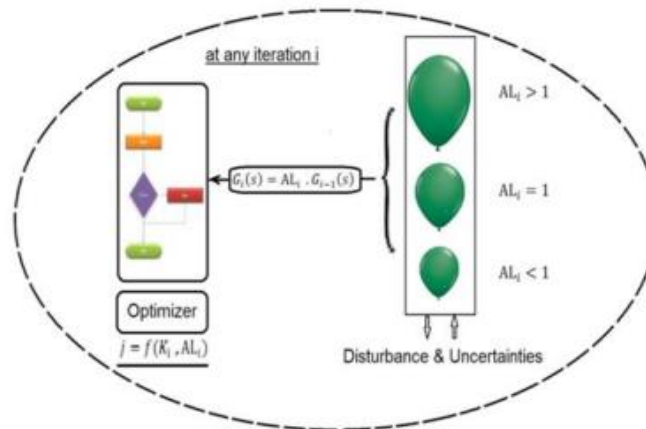


Figure 8. Optimization strategy-based Balloon Effect identifier [31], [32].

The online transfer function of the electric furnace temperature system for any iteration (i) will be:

$$G_i(s) = \frac{Y_i(s)}{U_i(s)} \quad (21)$$

Furthermore, $G_i(s)$ is a function of its previous value $G_{i-1}(s)$. AL_i stands for a gain and $G_0(s)$ represents the nominal process transfer function.

$$G_i(s) = AL_i G_{i-1}(s) \quad (22)$$

$$G_{i-1}(s) = \rho_i G_0(s) \quad (23)$$

where

$$\rho_i = \prod_{n=1}^{i-1} AL_n \quad (24)$$

$$G_i(s) = AL_i \rho_i G_0(s) \quad (25)$$

5. GTO-Based BE Identifier

Equation (2) describes the second-order transfer function plus the time delay for the electric furnace temperature system. By neglecting the time delay, Equation (2) is reduced to be:

$$G(s) = \frac{0.15}{s^2 + 1.1s + 0.2} \quad (26)$$

The lag compensator is chosen to provide a satisfactory tracking and regulating response of the electric furnace temperature control system. The transfer function of the lag compensator $G_c(s)$ will be:

$$G_c(s) = \frac{k_i(s+0.24)}{s} \quad (27)$$

Figure 9 shows the block diagram of the electric furnace temperature system controlled by an adaptive lag compensator using GTO-based Balloon Effect identifier. The GTO technique is used to determine the online transfer function of the electric furnace temperature system $G_i(s)$ for any iteration (i). However, the transfer function of the closed loop of the electric furnace temperature system is:

$$T.F(s) = \frac{G_i(s)G_c(s)}{1+G_i(s)G_c(s)H(s)} = \frac{\omega_n^2}{s^2 + 2\mu\omega_n s + \omega_n^2} \quad (28)$$

where $H(s)$ is a negative unity feedback transfer function and $G_i(s)$ depends on the transfer function of the electric furnace temperature system $G(s)$, which is called the nominal process transfer function, as explained below:

$$G_i(s) = AL_i \rho_i G_0(s) = \frac{0.15 * AL_i * \rho_i}{s^2 + 1.1s + 0.2}$$

Then, the characteristic equation in Equation (28) will be:

$$1 + G_i(s)G_c(s)H(s) = s^2 + 2\mu\omega_n s + \omega_n^2 = s^2 + 0.82s + 0.15 * AL_i * \rho_i * k_i$$

So,

$$\omega_n = \sqrt{0.15 * AL_i * \rho_i * k_i}, \quad \eta = \frac{0.82}{2\omega_n} \quad (29)$$

$$T_r = \frac{\pi - \sqrt{(1-\eta^2)}}{\omega_n \sqrt{(1-\eta^2)}}, \quad T_s = \frac{4}{\eta\omega_n}, \quad M_p = e^{\frac{-\pi\eta}{\sqrt{(1-\eta^2)}}} \quad (30)$$

The objective function of GTO based Balloon Effect identifier is chosen as:

$$J = \min \sum (T_r + T_s + M_p) \quad (31)$$

This means that The objective function J is a function of AL_i and k_i to address the system challenges.

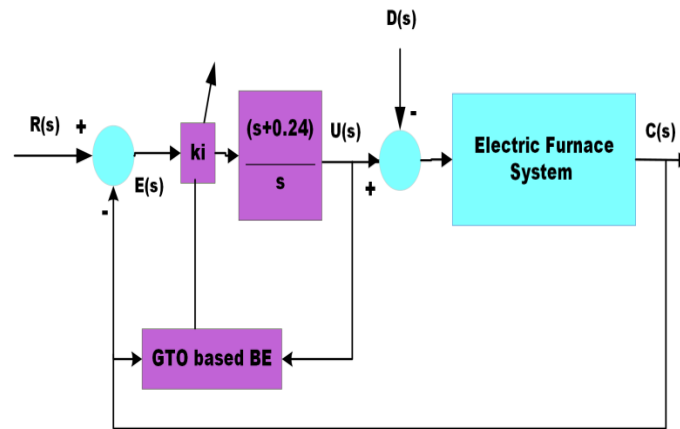


Figure 9. EF temperature system with GTO+BE.

6. Results and Discussion

In this part, the simulation results for the investigated three techniques are presented along with a comparison of their dynamic performance using the same circumstances. The three techniques are the adaptive lag compensator based on GTO+BE (C), MoFPA-based PID controller (C1) [10], and MoFPA-based PIDA controller (C2) [10]. All of C, C1, and C2 are designed and implemented for control of EF temperature. This control process aims to energy efficiency. The MATLAB/Simulink software is used to prove the efficacy and superiority of the proposed control scheme over other recent controllers.

6.1. First Scenario

With a constant temperature desired value, the dynamic performance of C for the EF temperature system is investigated in this scenario. Figure 10 explains the dynamic performance of C, C2, and C1 techniques. With C1, the dynamic performance rises at 4.1 s, reaches the steady state at 24 s, and has the maximum percent overshoot (M_p) about 18%. Moreover, the system dynamic performance with C2 rises at 7.5 s approximately and yields settling time (t_s) = 24 s and M_p = 5%. However, the dynamic response of the EF temperature system with C gives t_r = 2.9 s, t_s = 11 s, and M_p = 9%, as shown in Table 1. As a result, C generates a fast response and goes to a settling state quickly. So, the proposed C provides a satisfactory tracking and regulating response of the EF-TC system.

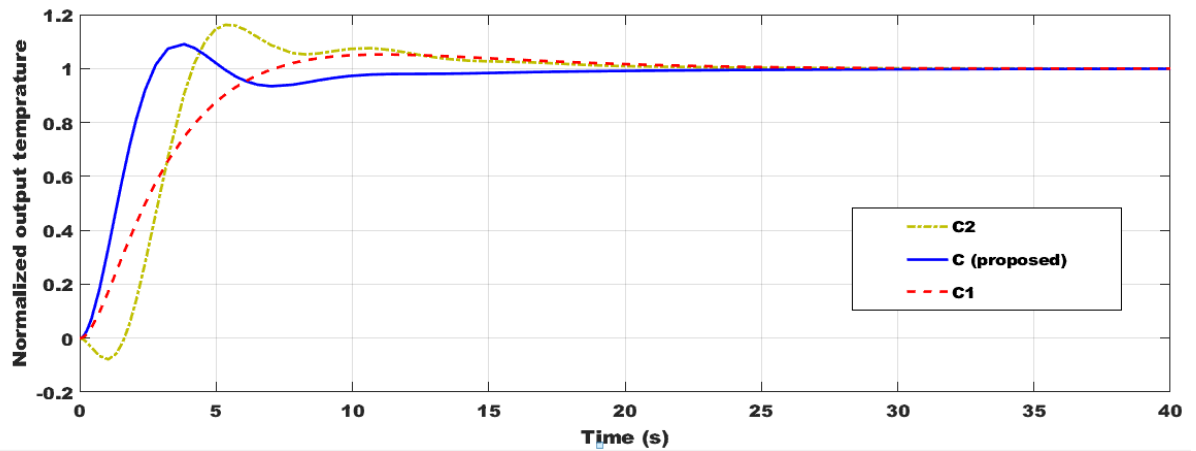


Figure 10. The dynamic performance of the EF under a constant temperature desired value.

Table 1. First scenario: performance evaluation.

Parameters	Investigated techniques		
	C1	C2	C (proposed)
t_r	4.1 s	7.5 s	2.9 s
t_s	24 s	24 s	11 s
M_p	18%	5%	9%

6.2. Second Scenario

In this case, the dynamic response of the EF temperature system with the different controllers is examined with a step change in the desired temperature at 20 s. The dynamic responses of the EF temperature system with C, C2, and C1 are compared as presented in Figure 11. The dynamic response with the C1 yields a maximum kick at 23 s, with the C2 provides a slow response, and the proposed C generates the best response, which is the fast performance with minimum undershoot at 25 s and reaches steady state at 30 s as explained in Table 2.

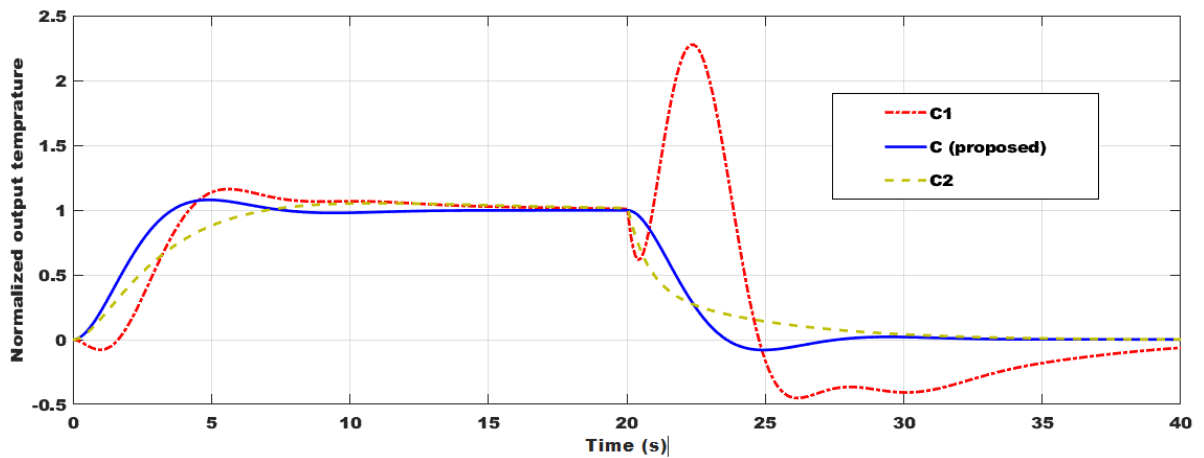


Figure 11. The dynamic performance of the EF under a step change in the desired temperature

Table 2. Second scenario: performance evaluation.

Parameters	Investigated techniques		
	C1	C2	C (proposed)
t_r	7.1 s	4 s	3.2 s
t_s	20 s	20 s	10 s
Undershoot	49%	-	9%

6.3. Third Scenario

The performance of the EF temperature system is surveyed under a step disturbance as shown in Figure 12. The performances of the studied system vary between 0.79 p.u. and 1.19 p.u. with C1, 0.85 p.u. and 1.12 p.u. with C2, 0.82 p.u. and 1.15 p.u. with the proposed C. In Figure 13, the dynamic performances of the studied system are explained, as where the best and fastest dynamic performance in tracking the desired value is with the proposed C.

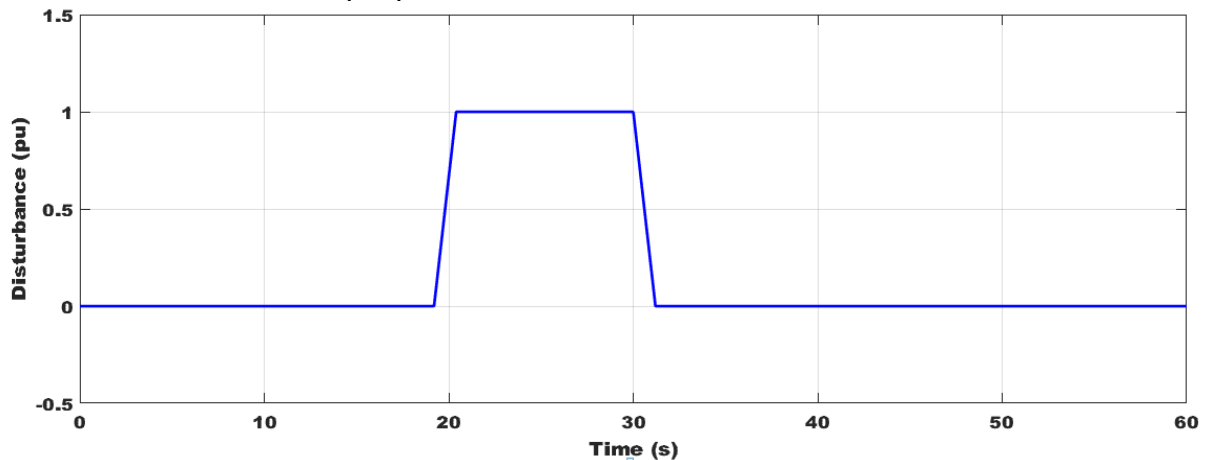


Figure 12. Step disturbance.

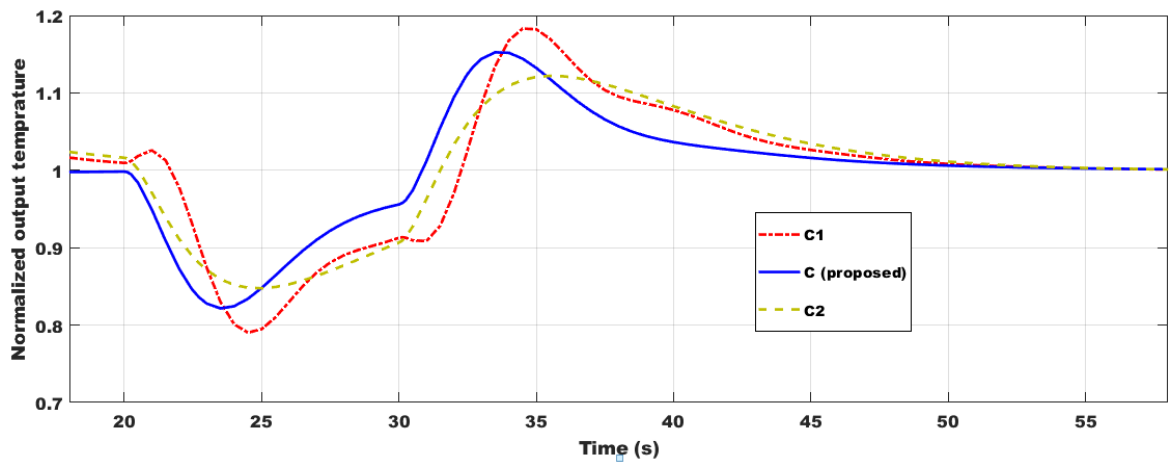


Figure 13. The dynamic performance of the EF under a step disturbance

6.4. Fourth Scenario

The dynamic response of the EF temperature system with the different controllers is examined with a random change in the desired temperature as shown in Figure 14. In Figure 15, the dynamic performances of the studied system are explained, as where the best performance is with the proposed C.

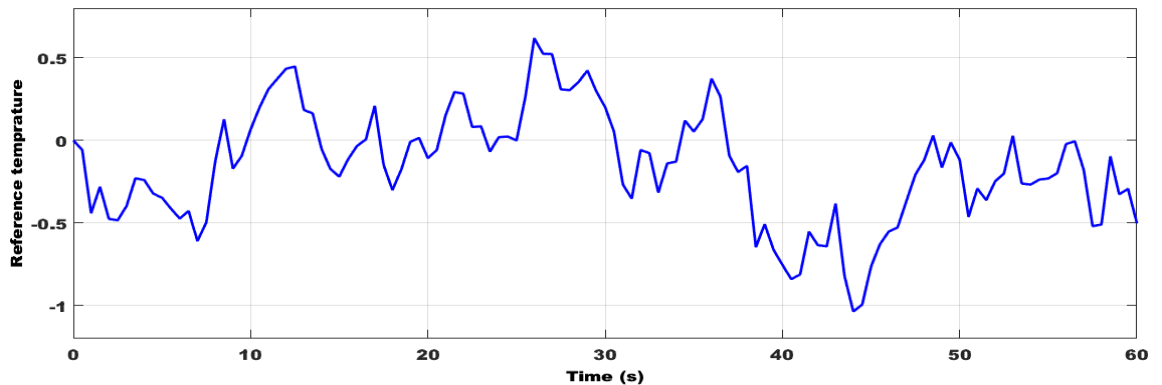


Figure 14. Random reference temperature

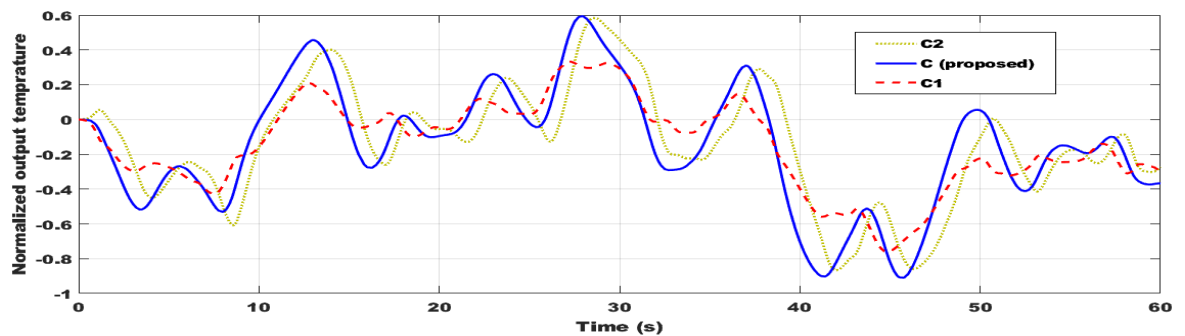


Figure 15. The dynamic performance of the EF with the three techniques under random

7. Conclusions

In industrial engineering applications, automatic control systems are typically tuned via a heuristic method that relies on the control engineer's knowledge and iterations of trial and error. In the end, EF's performance is acceptable but not ideal. In this sense, the primary purpose of this article is the design and validation of an advanced control strategy at the early design stage of the EF to achieve three objectives: (1) to reduce controller tuning time during EF commissioning, (2) to enhance EF performance in comparison to conventional industrial controllers, and (3) to lower system energy costs. Three control schemes (C, C1, and C2) are compared in MATLAB Simulink to validate the performance of C. Both C1 and C2 are chosen due to their industrial use.

The C method demonstrates the best performance and actuation balance when four simulation tests are taken into account, and C2 is superior to C1. Using a data set from the EF setup case results in a significant offset from the target, which results in excessive tracking errors in both tests. Finally, it can be concluded that, in comparison to C1 and C2, C enhances temperature tracking performance with the minimum overshoot, rise time, and settling time.

References

- [1] X. Hu, Q. Zou, and H. Zou, "Design and Application of Fractional Order Predictive Functional Control for Industrial Heating Furnace," *IEEE Access*, vol. 6, pp. 66565–66575, 2018, doi: 10.1109/ACCESS.2018.2878554.
- [2] X. Hu, H. Zou, J. Tao, and F. Gao, "Multimodel Fractional Predictive Functional Control Design with Application on an Industrial Heating Furnace," *Ind. Eng. Chem. Res.*, vol. 57, no. 42, pp. 14182–14190, 2018, doi: 10.1021/acs.iecr.8b03741.
- [3] Y. H. Duan, "The design of predictive fuzzy-PID controller in temperature control system of electrical heating furnace," in *Lecture Notes in Computer Science (including subseries Lecture Notes in Artificial Intelligence and Lecture Notes in Bioinformatics)*, 2010, vol. 6329 LNCS, no. PART 2, pp. 259–265. doi: 10.1007/978-3-642-15597-0_29.
- [4] J. C. Tudon-Martinez, J. D. J. Lozoya-Santos, A. Cantu-Perez, and A. Cardenas-Romero, "Advanced Temperature Control Applied on An Industrial Box Furnace," *J. Therm. Sci. Eng. Appl.*, vol. 14, no. 6, 2022, doi: 10.1115/1.4052020.
- [5] W. Tan, J. Liu, T. Chen, and H. J. Marquez, "Comparison of some well-known PID tuning formulas," *Comput. Chem. Eng.*, vol. 30, no. 9, pp. 1416–1423, 2006, doi: 10.1016/j.compchemeng.2006.04.001.
- [6] W. Der Chang, "A multi-crossover genetic approach to multivariable PID controllers tuning," *Expert Syst. Appl.*, vol. 33, no. 3, pp. 620–626, 2007, doi: 10.1016/j.eswa.2006.06.003.
- [7] U. S. Banu and G. Uma, "ANFIS gain scheduled CSTR with genetic algorithm based pid minimizing integral square error," in *IET Seminar Digest*, 2007, vol. 2007, no. 2, pp. 57–62. doi: 10.1049/ic:20070587.
- [8] N. B. Almutairi and M. Zribi, "Sliding mode controllers for a tempered glass furnace," *ISA Trans.*, vol. 60, pp. 21–37, 2016, doi: 10.1016/j.isatra.2015.11.005.
- [9] K. Rsetam, M. Al-Rawi, and Z. Cao, "Robust composite temperature control of electrical tube furnaces by using disturbance observer," *Case Stud. Therm. Eng.*, vol. 30, 2022, doi: 10.1016/j.csite.2022.101781.

- [10] N. Pringsakul and D. Puangdownreong, "Mofpa-based pida controller design optimization for electric furnace temperature control system," *Int. J. Innov. Comput. Inf. Control*, vol. 16, no. 6, pp. 1863–1876, 2020, doi: 10.24507/ijicic.16.06.1863.
- [11] R. Zhang, Q. Zou, Z. Cao, and F. Gao, "Design of fractional order modeling based extended non-minimal state space MPC for temperature in an industrial electric heating furnace," *J. Process Control*, vol. 56, pp. 13–22, 2017, doi: 10.1016/j.jprocont.2017.05.003.
- [12] D. Rawat, K. Bansal, and A. K. Pandey, "LQR and PID design technique for an electric furnace temperature control system," in *Advances in Intelligent Systems and Computing*, 2017, vol. 479, pp. 561–567. doi: 10.1007/978-981-10-1708-7_64.
- [13] H. Yu, J. Jia, G. Chen, and X. Chen, "Temperature control of electric furnace based on fuzzy PID," in *ICEOE 2011 - 2011 International Conference on Electronics and Optoelectronics, Proceedings, 2011*, vol. 3. doi: 10.1109/ICEOE.2011.6013295.
- [14] H. Z. Wang, H. R. Yang, and H. J. Chang, "Research and Design of the Temperature Control System of Crystal Annealing Furnace," *Appl. Mech. Mater.*, vol. 697, pp. 285–288, 2014, doi: 10.4028/www.scientific.net/amm.697.285.
- [15] D. Du Wen, "Decoupling control of electric heating furnace temperature based on DRNN neural network," in *ICECT 2010 - Proceedings of the 2010 2nd International Conference on Electronic Computer Technology*, 2010, pp. 261–264. doi: 10.1109/ICECTECH.2010.5479934.
- [16] D. Sain, S. K. Swain, S. K. Mishra, and S. Dutta, "Robust set-point weighted PID controller design using genetic algorithm for electric furnace temperature control system," *Int. J. Control Theory Appl.*, vol. 9, no. 39, pp. 29–36, 2016.
- [17] M. M. Gani, M. S. Islam, and M. A. Ullah, "Optimal PID tuning for controlling the temperature of electric furnace by genetic algorithm," *SN Appl. Sci.*, vol. 1, no. 8, 2019, doi: 10.1007/s42452-019-0929-y.
- [18] X. Peng, Z. Mo, and S. Xie, "Research and application on two-stage fuzzy neural network temperature control system for industrial heating furnace," *J. Comput.*, vol. 7, no. 2, pp. 433–438, 2012, doi: 10.4304/jcp.7.2.433-438.
- [19] D. Shi, G. Gao, Z. Gao, and P. Xiao, "Application of expert fuzzy PID method for temperature control of heating furnace," in *Procedia Engineering*, 2012, vol. 29, pp. 257–261. doi: 10.1016/j.proeng.2011.12.703.
- [20] S. Alghamdi et al., "Optimal PID Controllers for AVR Systems Using Hybrid Simulated Annealing and Gorilla Troops Optimization," *fractal Fract.*, vol. 6, no. 11, p. 682, 2022, [Online]. Available: <https://doi.org/10.3390/fractalfract6110682>
- [21] M. Ali, H. Kotb, K. M. Aboras, and N. H. Abbasy, "Design of cascaded pi-fractional order PID controller for improving the frequency response of hybrid microgrid system using gorilla troops optimizer," *IEEE Access*, vol. 9, pp. 150715–150732, 2021, doi: 10.1109/ACCESS.2021.3125317.
- [22] S. S. Kareem, R. R. Mostafa, F. A. Hashim, and H. M. El-Bakry, "An Effective Feature Selection Model Using Hybrid Metaheuristic Algorithms for IoT Intrusion Detection," *Sensors*, vol. 22, no. 4, 2022, doi: 10.3390/s22041396.
- [23] A. Ramadan, M. Ebeed, S. Kamel, A. M. Agwa, and M. Tostado-véliz, "The Probabilistic Optimal Integration

- of Renewable Distributed Generators Considering the Time-Varying Load Based on an Artificial Gorilla Troops Optimizer,” *Energies*, vol. 15, no. 4, 2022, doi: 10.3390/en15041302.
- [24] A.-A. A. Mohamed, A. A. M. El-Gaafary, Y. S. Mohamed, and A. M. Hemeida, “Design static VAR compensator controller using artificial neural network optimized by modify Grey Wolf Optimization,” 2015 International Joint Conference on Neural Networks (IJCNN). IEEE, Jul. 2015. doi: 10.1109/ijcnn.2015.7280704.
- [25] A.-A. A. Mohamed, A. L. Haridy, and A. M. Hemeida, “The Whale Optimization Algorithm based controller for PMSG wind energy generation system,” 2019 International Conference on Innovative Trends in Computer Engineering (ITCE). IEEE, Feb. 2019. doi: 10.1109/itce.2019.8646353.
- [26] A. Ginidi, S. M. Ghoneim, A. Elsayed, R. El-Sehiemy, A. Shaheen, and A. El-Fergany, “Gorilla troops optimizer for electrically based single and double-diode models of solar photovoltaic systems,” *Sustain.*, vol. 13, no. 16, 2021, doi: 10.3390/su13169459.
- [27] B. Abdollahzadeh, F. Soleimani Gharehchopogh, and S. Mirjalili, “Artificial gorilla troops optimizer: A new nature-inspired metaheuristic algorithm for global optimization problems,” *Int. J. Intell. Syst.*, vol. 36, no. 10, pp. 5887–5958, 2021, doi: 10.1002/int.22535.
- [28] M. Abdel-Basset, D. El-Shahat, K. M. Sallam, and K. Munasinghe, “Parameter extraction of photovoltaic models using a memory-based improved gorilla troops optimizer,” *Energy Convers. Manag.*, vol. 252, 2022, doi: 10.1016/j.enconman.2021.115134.
- [29] N. Hassan and A. Saleem, “Neural Network-Based TID Controller for Wheeled Mobile Robot Trajectory Tracking,” in *Lecture Notes in Networks and Systems*, 2022, vol. 235, pp. 207–215. doi: 10.1007/978-981-16-2377-6_21.
- [30] S. Das, L. C. Saikia, and S. Datta, “Maiden application of TIDN-(1+PI) cascade controller in LFC of a multi-area hydro-thermal system incorporating EV–Archimedes wave energy-geothermal-wind generations under deregulated scenario,” *Int. Trans. Electr. Energy Syst.*, vol. 31, no. 7, 2021, doi: 10.1002/2050-7038.12907.
- [31] Y. A. Dahab, H. Abubakr, and T. H. Mohamed, “Adaptive load frequency control of power systems using electro-search optimization supported by the balloon effect,” *IEEE Access*, vol. 8, pp. 7408–7422, 2020, doi: 10.1109/ACCESS.2020.2964104.
- [32] T. H. Mohamed, M. A. M. Alamin, and A. M. Hassan, “Adaptive position control of a cart moved by a DC motor using integral controller tuned by Jaya optimization with Balloon effect,” *Comput. Electr. Eng.*, vol. 87, 2020, doi: 10.1016/j.compeleceng.2020.106786.
- [33] S. Jung and R. C. Dorf, “Analytic PIDA controller design technique for a third order system,” *Proceedings of the IEEE Conference on Decision and Control*, vol. 3. pp. 2355–3592, 1996. doi: 10.1109/cdc.1996.573472.